Preparation of novel composite VPO/fumed silica catalyst for partial oxidation of *n*-butane

Z.Q. Zhou, H.Y. Xu, W.J. Ji*, and Y. Chen

Key Laboratory of Mesoscopic Chemistry of the Ministry of Education, Department of Chemistry, Nanjing University, Nanjing 210093, P.R. China

Received 11 March 2004; accepted 3 May 2004

By applying fumed SiO_2 and the deposition–precipitation method based on organic medium, the composite VPO/fumed SiO_2 catalysts were first prepared and tried for partial oxidation of *n*-butane to maleic anhydride. In the temperature range of 653–693 K the fumed SiO_2-based catalysts not only showed good activity but also maintained sufficiently high MA selectivity in comparison to some conventional supported VPO catalysts. As an example, the catalyst with 30% VPO content showed butane conversion of 60% and MA selectivity of 58 mol% at 673 K. The turnover rates of low loading samples are found to be higher than that of high loading sample as well as unsupported catalyst. Besides the unique interaction which may exist between VPO component and the fumed SiO_2 material, co-existence of dominant $(VO)_2P_2O_7$ and minor $VOPO_4$ in these non-equilibrated catalysts may be favorable for MA formation. Moreover, introducing the additive of polyethylene glycol (PEG) in the preparation medium can obviously enhance the dispersion of VPO component and hence lead to a more selective catalyst.

KEY WORDS: fumed SiO_2; VPO; partial oxidation; *n*-butane; maleic anhydride.

1. Introduction

Selective oxidation of *n*-butane to maleic anhydride (MA) is currently the only commercialized process for light paraffin conversion, and the efficient catalysts primarily consist of unsupported vanadyl pyrophosphate, $(VO)_2P_2O_7$ [1,2]. Although this type of catalyst has been extensively studied for decades, still a full understanding of the reaction details is not thoroughly achieved. The form of active phase (amorphous versus crystallized) [3–6], the role of V^{5+} species [7–9], the surface enrichment of P element [10,11] and so on are the major aspects of debates. On the other hand, supporting VPO on various oxides has several potential advantages over unsupported one, and attempts to prepare supported VPO catalysts on different support materials have been tried [12–16]. These studies also provide supplementary information for understanding this complicated reaction. The introduction of support, however, may induce support–oxide interactions that could hinder the formation of the active $(VO)_2P_2O_7$ phase, and the resulted catalysts would exhibit low butane conversion and/or poor MA selectivity [17–19]. The type and/or nature of support materials also showed a significant influence on reaction performance. When there is a strong interaction between VPO and a reducible support, such as titania and zirconia, the VPO entities became more reducible, and enhancement in catalytic activity is remarkable; on the other hand, the application of a support such as silica that interacts less strongly with the active phase/species, would improve the selectivity but decrease the conversion [13,14]. Ruitenbeek *et al.* [20] made similar observations on a series of supported VPOs. The form of the supported VPO species was also found to be related to the P/V ratio of catalysts [12,13]. Supported VPO component would exist in the form of α_I-$VOPO_4$, α_{II}-$VOPO_4$ and $VOPO_4 \cdot xH_2O$ or amorphous state when the P/V ratio was 1.0 and greater than 2, respectively. In the latter case, higher MA selectivity (50%) can be achieved. It was also found that the state of supported VPO component would be influenced by the surface properties of SiO_2 support [16]. We previously prepared supported VPO catalysts on MCM-41 and SiO_2 of large pore [21,22], and found that the MCM-41-supported VPO specimen at an appropriate VPO loading showed considerably improved MA selectivity. The method and the medium (aqueous or organic) for catalyst preparation also showed a great effect on the behavior of the catalyst. In this study, we first adopted a unique kind of silica, namely, fumed SiO_2, to prepare novel composite VPO/fumed silica catalysts for the target reaction. Fumed silica is composed of non-porous primary particles. It has chain-like particle morphology and the only one porosity is that between the primary particles. One method for the production of fumed silica involved a continuous flame hydrolysis technique. It involves the conversion of silicon tetra chloride ($SiCl_4$) to the gas phase using an oxy hydrogen flame. It then reacts with water to yield silica (SiO_2) and hydrochloric acid.

---

*To whom correspondence should be addressed.
E-mail: jiwj@nju.edu.cn

1011-372X/04/0700–0221/0 © 2004 Plenum Publishing Corporation

In our previous study [23] the polyethylene glycol (PEG) was found to be effective in synthesizing highly active and selective VPOs; thus it was also adopted here to prepare a PEG-derived composite VPO/fumed SiO_2 for comparison. Herein we reported the results of characterization and evaluation of the series of catalysts.

2. Experimental

2.1. Catalyst preparation

The composite VPO/fumed SiO_2 catalysts with the wide range of VPO content (20–60 wt%) were prepared in this study. The fumed SiO_2 was purchased from Aldrich Chemical Company and used without further treatment. The deposition–precipitation method for catalyst preparation in an organic medium was found to be preferred in our previous studies [21,22]. Briefly speaking, the catalyst precursor was prepared in an organic medium by the reaction of V_2O_5 with a mixture of *iso*-butanol and benzyl alcohol (volume ratio of 1 : 1). After the reaction mixture was refluxed at 413 K for 5 h, certain amount of fumed SiO_2 material was introduced, and the reaction mixture was refluxed for 1 h. Then phosphoric acid was added drop wise at a vanadium/phosphorus atomic ratio of 1.0/1.2. After refluxing for another 6 h, the turbid reaction mixture was filtered. The resulted precipitate was washed several times with *iso*-butanol and acetone, respectively; then dried in air at 393 K for 24 h. The dried precursor was *in situ* activated in the mixture of 1.5% *n*-butane/air at a rate of 2 K/min from room temperature to 673 K and kept at this temperature for 15 h. For comparison, certain amount of PEG 20,000 was added into the preparation medium before the fumed SiO_2 was introduced, followed by the addition of phosphoric acid.

2.2. Characterization

The characterization of the freshly activated samples was conducted by means of BET, XRD, SEM, TEM and Raman measurements. Specific surface areas were measured by nitrogen adsorption–desorption at 77 K on the Sorptomatic 1900 apparatus (Carlo Erba Copporation, Italy). X-ray diffraction patterns were recorded at room temperature using a Shimadzu XD-3A diffraction meter with Graphite-filtered CuK_α radiation. X-ray tube was operated at 35–40 kV and 100–200 mA, respectively. The morphology of the samples and the distribution of VPO component were checked on a SEM-200 Scanning Electron Microscopy and a TEM-200CX Transmission Electron Microscopy (JEOL). Raman spectra were collected on a LABRAM-HR Raman spectrometer at room temperature with the excitation source of 513 nm and power of 1.5 mW.

2.3. Catalyst evaluation

Catalytic performance for partial oxidation of *n*-butane to MA was evaluated in a quartz fixed-bed micro-reactor ($\Phi = 8$ mm) with a continuous down-flow. The catalyst samples were pressed to pellets and then crushed and sieved. Typically, 0.5 g 25–40 mesh sample was used for the reaction. The feed composition was 1.5% n-C_4H_{10}, 17.5% O_2 and balanced N_2. The gas hourly space velocity (GHSV) was ca. 1200 h^{-1}. On-line gas chromatography system was used to analyze the outlet mixture; the carbon balance was usually better than 95%.

3. Results and discussion

The surface area of the fumed SiO_2 without any pretreatment such as dryness and calcination is 250 m^2/g, and those of the 20%-, 30%-, 40%-, 50%-, and 60%-VPO/fumed SiO_2 samples are 208, 176, 165, 160 and 130 m^2/g, respectively. Considering the effect of increasing content of VPO and decreasing content of the fumed SiO_2 in the sample series, the presence of VPO does not notably affect the surface area of fumed SiO_2. When looking at the variation of the BET surface area as a function of the VPO amount, the surface of samples will increase with increasing VPO content if the amount of silica is taken constant in the samples. This is due to the contribution of the VPO phase to the surface area. In fact, fumed silica is non-porous in the primary spherical particles, and the only one porosity is that between the primary particles. This porosity may also be spacious for the accommodation of VPO component. XRD results of the serial composite VPO/fumed SiO_2 samples are shown in figure 1. Even at low VPO content, the VPO component existed essentially in the form of $(VO)_2P_2O_7$ phase [11,24], which differs considerably from the observations made on the other supported

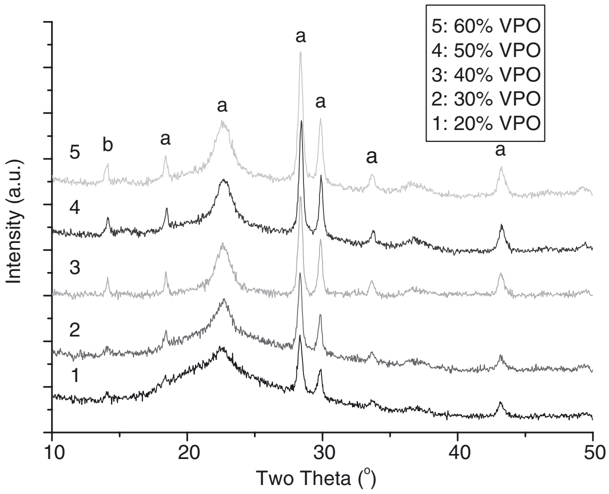

Figure 1. XRD patterns of various composite VPO/SiO_2 catalysts: a, $(VO)_2P_2O_7$; b, $VO(H_2PO_4)_2$.

VPO catalysts [12–16,21,22]. $\alpha\text{-VOPO}_4$, $\gamma\text{-VOPO}_4$ and $\text{VO(SiO)P}_2\text{O}_7$ phases could form in large quantities in the conventional SiO_2-supported VPO samples, especially when the samples were prepared in aqueous media [12,13,16]. Over the Al-containing MCM-41-supported samples, large portion of VPO component was found to be in amorphous form even at high loadings [21], and it is also the case if the VPO component was deposited on the silica support by an electrochemical mean [14,15]. On the SiO_2-supported sample of large pores, however, certain amount of $\text{(VO)}_2\text{P}_2\text{O}_7 \cdot \text{H}_2\text{O}$ phase could exist at high loadings [22]. The observed deviation is possibly due to large difference in texture and porosity between fumed SiO_2 and conventional SiO_2, SiO_2 of large pore as well as MCM-41. Besides the major $\text{(VO)}_2\text{P}_2\text{O}_7$ phase, there is minor $\text{VO(H}_2\text{PO}_4)_2$ phase existing in the fumed SiO_2-based samples. No V^{5+} phases are shown by XRD. Note that in the low loading samples the intensity of diffraction peak of the (200) plane significantly decreased and the peak width notably broadened, which could be owing to more severe structural disorder of VPO species and the contribution of the silica support. Interestingly, in the higher loading samples the diffraction intensity and the peak width of the (200) plane can also be noticeably influenced when extra amount of *iso*-butanol and benzyl alcohol was used for catalyst preparation, seen in figure 2 (3 and 4). Since the content of fumed SiO_2 in these two samples is the same, thus the broadening of the (200) peak is not a result of the contribution of silica support, but a distinguished structural disorder alone this plane. This structural disorder may be induced by alcohol intercalation into the VPO precursor. On the contrary, adding the agent of PEG in the preparation medium seems not to affect the local structure of VPO component obviously, seen in figure 2 (1 and 2).

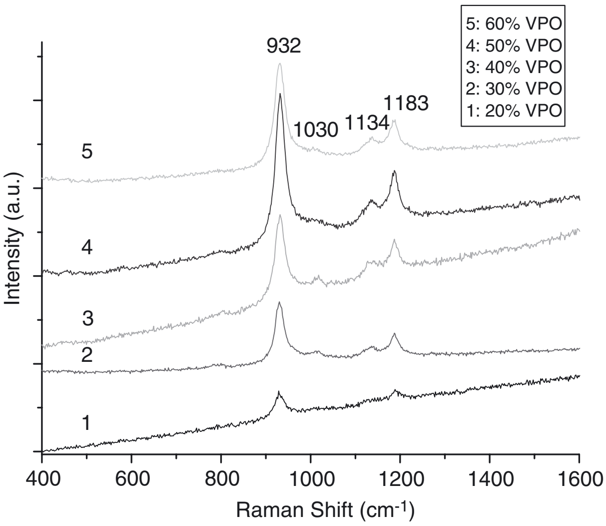

Figure 3. Raman spectra of the VPO/fumed SiO_2 catalysts with different VPO content.

The Raman spectra of the representative samples are presented in figure 3. It is found that the Raman signals are rather weak for the low loading samples, which may be due to the nature of fumed SiO_2 material. The signals increased with increasing VPO content and the bands at 930, 1030, 1134 and 1183 cm^{-1} can be distinguished, among them the major band at ca. 930 cm^{-1} could be due to the $\nu_{\text{as, P–O–P}}$ in the $\text{P}_2\text{O}_7^{2-}$ unit of $\text{(VO)}_2\text{P}_2\text{O}_7$, and the weak bands at ~1130 and ~1180 cm^{-1} are the characteristics of the $\text{(VO)}_2\text{P}_2\text{O}_7$ phase [25,26]. It is evident by more sensitive Raman spectroscopy that small amount of VOPO_4 does exist in the samples, since

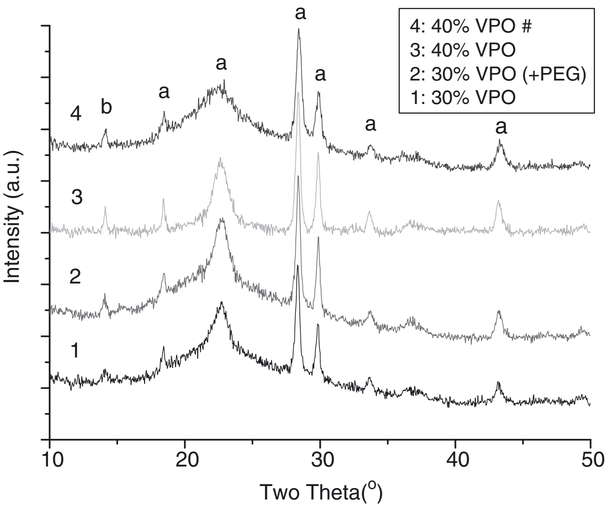

Figure 2. Comparison of XRD patterns of the composite VPO/SiO_2 catalysts synthesized via modified preparation procedures: a, $\text{(VO)}_2\text{P}_2\text{O}_7$; b, $\text{VO(H}_2\text{PO}_4)_2$. Sample 2 was prepared in the presence of PEG while sample 4 (#) was prepared via the reaction of V_2O_5 with extra alcohols.

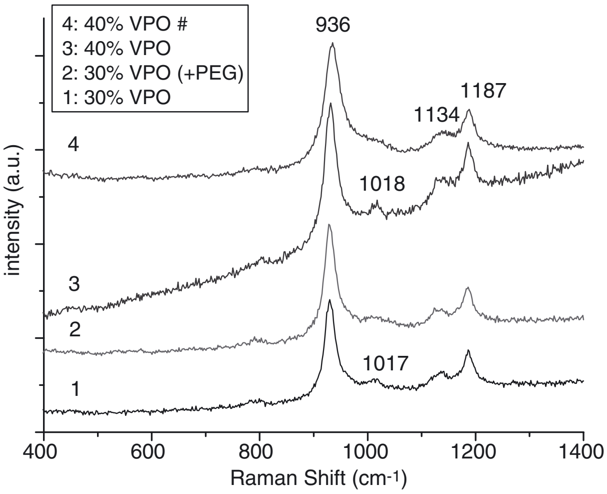

Figure 4. Comparison of Raman spectra of the VPO/fumed SiO_2 samples synthesized via modified preparation procedures. Sample 2 (+PEG) and sample 4 (#) were prepared in the presence of PEG and with extra alcohols, respectively.

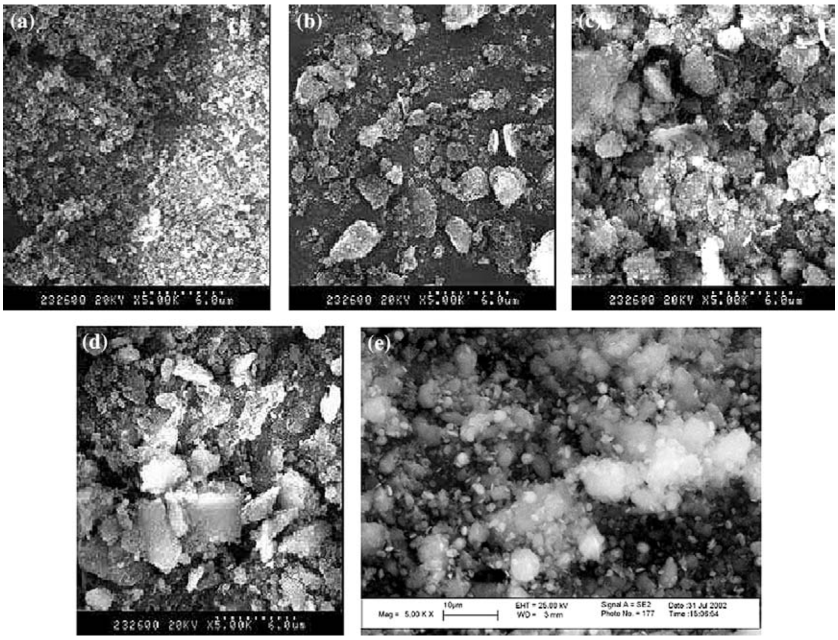

Figure 5. SEM photographs of (a) fumed SiO_2 support, (b) 20%-, (c) 30%-, (d) 50%-VPO/fumed SiO_2 and (e) PEG-derived 28%-VPO/fumed SiO_2.

there is broadened and weak shoulder/peak at 1017–1030 cm^{-1} which is the characteristic of $VOPO_4$. Because of its low concentration, it is hardly shown by XRD. It is recognized that the presence of $VOPO_4$ is likely due to the fact that the samples are subjected to a relatively short calcination process and still non-equilibrated as compared to the equilibrated ones subjected to a few weeks long calcination on stream. It was also found that less $VOPO_4$ was formed when excess amount of alcohols or the PEG agent was applied in the preparation medium, seen in figure 4. These are in agreement with the X-ray power data and also consistent with our previous observation made on the PEG-derived unsupported VPOs [27].

The SEM photographs indicated the morphology of the obtained composite VPO/fumed SiO_2 samples (figure 5). The block species are recognized as the VPO component. It is clearly that the quantity of VPO particles on the surface increased with VPO content, meanwhile the average particle size of supported VPO component also apparently enlarged. Interestingly, the PEG-derived sample showed a quite different picture. It was clearly observed in figure 5 that under comparable magnification the average particle size of the VPO component (the small plate-form species) in the PEG-derived sample decreased considerably; and the particle size of the VPO specimen still changed insignificantly at high VPO content (not shown), suggesting in the PEG-derived sample the VPO component is more uniformly dispersed. TEM investigation of the selected samples was also conducted and one of the photographs was presented in figure 6. It seems that the VPO component may not only exist outside the aggregated particles but also be enclosed inside the porosity between the primary particles.

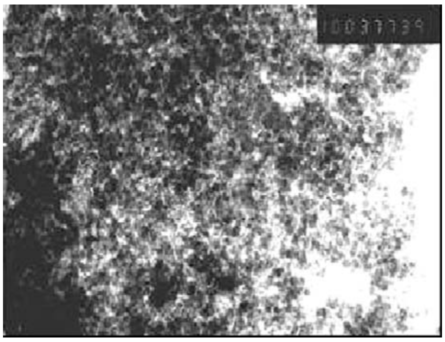

Figure 6. TEM photograph of 30%-VPO/fumed SiO_2 catalyst. Magnifying 100,000×.

The catalytic performance for partial oxidation of *n*-butane to MA over these fumed SiO_2-based VPOs was evaluated and the results were summarized in table 1. Note that these derived catalysts are not only active but rather selective as well for the target reaction, giving the pronounced yield of MA as compared with some conventional supported VPO catalysts reported [14,15,20]. For example, the typical performance obtained at 673 K on the 30% VPO/fumed SiO_2 sample is 60% of *n*-butane conversion and 58 mol% of MA selectivity. This attractively good performance is partly thanks to the fact that certain phase composition is obtained in the fumed SiO_2-based samples. From table 1, butane conversion apparently increased with increasing VPO loading and reaction temperature, but the increment due to elevating temperature is more notable. On the other hand, MA selectivity rapidly

Table 1
The reaction performances of the VPO/fumed SiO_2 catalysts

Sample	Temp. (K)	Conv. (%)	Sel. (mol%)	Yield (mol%)	Specific activity (μmol/g(VPO) Min[a])
20%-loading	653	29	54	16	19.6
	673	41	50	21	27.1
	693	56	46	26	33.2
30%-loading	653	44	61	27	22.6
	673	60	57	34	28.6
	693	77	48	37	31.7
40%-loading	653	51	66	34	21.1
	673	69	59	41	25.6
	693	86	50	43	27.1
50%-loading	653	58	66	38	19.6
	673	76	61	46	22.6
	693	91	51	46	22.6
60%-loading	653	61	66	40	16.6
	673	81	59	48	19.6
	693	95	49	47	19.6

[a] The activity was normalized to per unit mass of VPO loading.

decreased at higher temperatures but slightly increased with increasing VPO loading. The catalysts showed fairly high butane conversion and meanwhile maintained comparatively good MA selectivity and consequently led to a high level of MA yield. The data of specific activity (normalized to per unit mass of VPO loading) revealed that the catalyst performance is essentially decreased with increasing VPO loading, indicating the character of VPO component should vary somehow with the VPO content in the sample. This deduction was also supported by comparison of the turnover rates as well as MA selectivity for the composite VPO/fumed SiO_2 and unsupported catalyst at 673 K, seen in table 2. It reveals that higher intrinsic activity is obtained on the low loading samples and this trend is in agreement with the specific activities listed in table 1. The deviation in turnover rates (TORs) and MA selectivity further suggested that the nature of VPO component not only change with the VPO content in the fumed SiO_2 based samples but also be different from that of unsupported VPO catalyst. The PEG-derived catalyst, however, behaved quite differently and the comparison was made in figure 7. Clearly, this catalyst is much more selective but less active than the non-PEG-derived one. Such difference is likely attributable to obviously different dispersion state of the VPO species, and the varied interaction between the supported VPO component and fumed SiO_2 material. The presence of PEG molecules may decrease the surface energy of nucleation of $VO(HPO_4) \cdot 0.5H_2O$ precursor and promote uniform precipitation of the fine $VO(HPO_4) \cdot 0.5H_2O$ particles. The PEG molecule adsorbed on the precursor surface may also effectively hinder agglomeration of the fine precursor particles. The gradual removal of PEG resident at the precursor surface in the following activation procedure is likely beneficial in generating highly dispersed $(VO)_2P_2O_7$. It is worth to note that increasing the ratio of alcohols to vanadium oxide in preparation medium could also give rise to a remarkable impact on the reaction performance of final catalyst, seen in table 3. Assuming the dispersion of VPO in these two catalysts is similar, and then the major differences between the two samples are the local crystalline structure and the content of $VOPO_4$ as

Table 2
Comparsion of the TORs and MA selectivity for the VPO/fumed SiO_2 samples and unsupported catalyst at 673 K

Sample	20%-loading	40%-loading	60%-loading	Unsupported
TORs[a] (μmol m^{-2}(VPO) min^{-1})	0.68	0.56	0.39	0.52
MA selectivity (mol%)	50	59	59	65

[a] Surface area of VPO was calculated by subtracting the surface area of silica from that of the catalyst.

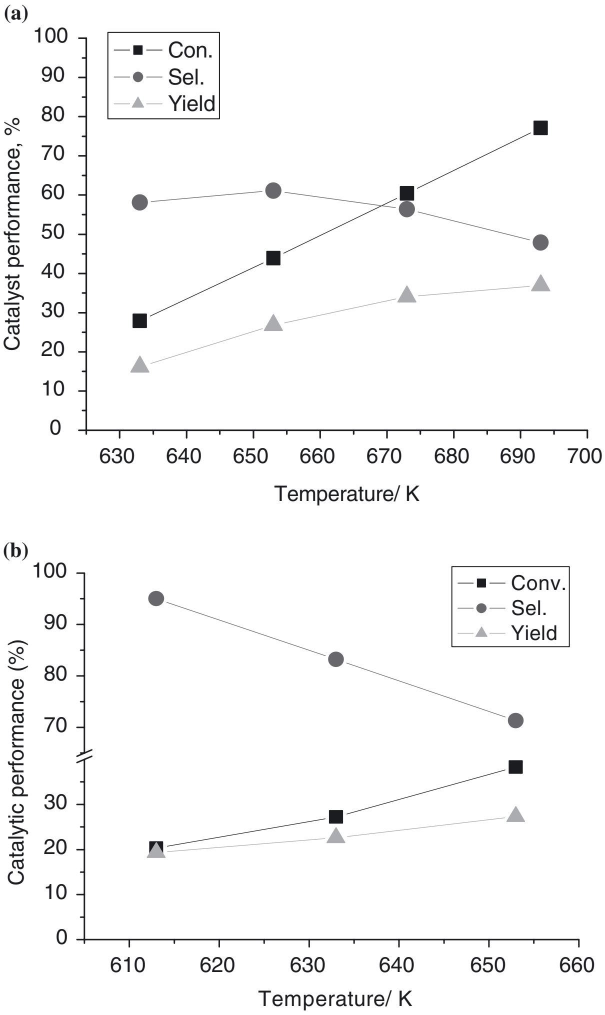

Figure 7. Comparison of the reaction performances on (a) 30%-VPO/fumed SiO_2 and (b) PEG-derived 28%-VPO/fumed SiO_2.

Table 3
The performances of the two VPO/fumed SiO_2 catalysts with 40% loading

Sample	Temp. (K)	Conv. (%)	Sel. (mol%)	Yield (%)	Specific activity (μmol/g(VPO) min)
40%-VPO	673	69	59	41	25.6
	693	86	50	43	27.1
40%-VPO[a]	673	55	44	24	15.1
	693	73	39	28	18.1

[a] The catalyst was prepared via the reaction of extra alcohols with V_2O_5.

revealed by XRD and Raman results (figures 2 and 4). Additional amount of alcohols used in the preparation medium may have alcohol intercalation into VPO precursor which induces structural disorder. Moreover, additional alcohol probably results in a deeper reduction of V^{5+} during precursor synthesis, and these are the possible reasons for the declined reaction performance (seen in table 3). In conclusion, in teams of the achieved level of butane conversion and MA selectivity, the fumed SiO_2-based catalysts are superior to most of conventional supported VPO catalysts reported for the target reaction. A dominant $(VO)_2P_2O_7$ phase together with certain amount of $VOPO_4$ can be obtained in the fumed SiO_2-based samples, which may be the result of unique nature of the fumed SiO_2 and the interaction between VPO component and the adopted support. In the non-equilibrated catalyst both $(VO)_2P_2O_7$ and $VOPO_4$ were found to be important for the catalyst performance [8,28,29]. Our results obtained on the serial PEG-derived unsupported VPOs also display a similar tendency [30]. In addition, the local structural disorder and the possibly changed exposure along the (200) crystal plane evident by substantial broadening of diffraction peak in the low loading sample may also be relevant to MA formation [31,32].

Acknowledgments

We acknowledge the financial supports from the Ministry of Science and Technology of China (G2000048009), Natural Science Foundation of Jiangsu Province (BK2001202) and the High-Tech Project of Jiangsu Province (BG2001038).

References

[1] B.K. Hodnett, Catal. Rev.-Sci. Eng. 27 (1985) 373.

[2] G. Centi, F. Trifiro, J.R. Ebner and V.M. Franchetti, Chem. Rev. 88 (1988) 55.

[3] A. Bruckner, B. Kubias and B. Lucke, Catal. Today 32 (1996) 215.

[4] V.V. Guliants, S.A. Holmes, J.B. Benziger, P. Heaney, D. Yates and I.E. Wachs, J. Mol. Catal. A: Chem. 172 (2001) 265.

[5] G.J. Hutchings, J.K. Bartley, J.M. Wester, J.A. Lopez-Sanchez, D.J. Gilbert, C.J. Kiely, A.F. Carley, S.M. Howdle, S. Sajip, S. Caldarelli, C. Rhodes, J.C. Volta and M. Poliakoff, J. Catal. 197 (2001) 232.

[6] G.J. Hutchings, J.A. Lopez-Sanchez, J.K. Bartley, J.M. Wester, A. Burrows, C.J. Kiely, A.F. Carley, C. Rhodes, M. Havecker, A. Knop-Gericke, R.W. Mayer, R. Schlogl, J.C. Volta and M. Poliakoff, J. Catal. 208 (2002) 197.

[7] V.V. Guliants, J.B. Benziger, S. Sundaresan, N. Yao and I.E. Wachs, Catal. Lett. 32 (1995) 379.

[8] G.J. Hutchings, A.D. Chomel, R. Olier and J.C. Volta, Nature 368 (1994) 41.

[9] G.W. Coulston, S.R. Bare, H.H. Kung, K.E. Birkeland, G.K. Bethke, R. Harlow, N. Herron and P.L. Lee, Science 275 (1997) 191.

[10] L.M. Cornaglia, C. Caspani and E.A. Lombardo, Appl. Catal. 74 (1991) 15.

[11] P. Delichere, K.E. Bere and M. Abon, Appl. Catal. A: Gen. 172 (1998) 295.

[12] W.D. Harding, K.E. Birkeland and H. H. Kung, Catal. Lett. 28 (1994) 1.

[13] K.E. Birkeland, S.M. Babitz, G.K. Bethke, H.H. Kung, G.W. Coulston and S.R. Bare, J. Phys. Chem. B 101 (1997) 6895.

[14] R.A. Overbeek, A.R.C.J. Pekelharing, A.J. van Dillen *et al.*, Appl. Catal. A 135 (1996) 231.

[15] R.A. Overbeek, P.A. Warringa, M.J.D. Combag *et al.*, Appl. Catal. A 135 (1996) 209.

[16] J.M.C. Bueno, G.K. Bethke, M.C. Kung and H.H. Kung, Catal. Today 43 (1998) 101.

[17] V.A. Zazhigalov, Y.P. Zaitsev, V.M. Belousov, B. Parlitz, W. Hanke and G. Ohlman, React. Kinet. Catal. Lett. 32 (1986) 209.

[18] N.T. Do and M. Baerns, Appl. Catal. 45 (1988) 1.

[19] N.T. Do and M. Baerns, Appl. Catal. 45 (1988) 9.

[20] M. Ruitenbeck, A.J. van Dillen, A. Barbon, E.E. van Faassen, D.C. Koningsberger and J.W. Geus, Catal. Lett. 55 (1998) 133.

[21] W. Nie, X. Wang, W. Ji, Q. Yan, Y. Chen and C.T. Au, Catal. Lett. 76 (2001) 201.

[22] W. Nie, Z. Wang, W. Ji, Q. Yan, Y. Chen and C.T. Au, Appl. Catal. A: Gen. 244 (2003) 265.

[23] X. Wang, L. Xu, X. Chen, W. Ji, Q. Yan and Y. Chen, J. Mol. Catal. A: Chem. 206 (2003) 201.

[24] H. Igarashi, K. Tsuji, T. Okuhara and M. Misono, J. Phys. Chem. 97 (1993) 7065.

[25] A.F. Ben, R. Oliver, N. Guillaume, F. Lefebvre and J.C. Volta, J. Catal. 134 (1992) 151.

[26] V.V. Guliants, J.B. Benziger, S. Sundaresan, I.E. Wachs, J.M. Jehng and J.E. Roberts, Catal. Today 28 (1996) 275.

[27] W. Ji, X. Wang, Q. Yan and Y. Chen, in: 18th North American Catalysis Society Meeting, Cancun, June 1–6, 2003.

[28] M.T. Sananes-Schulz, A. Tuel, G.J. Hutchings and J.C. Volta, J. Catal. 166 (1997) 388.

[29] E. Bordes, Catal. Today 16 (1993) 27.

[30] X. Wang, X. Chen, W. Ji, B. Li, Q. Yan and Y. Chen, J. Phys. Chem. B, to be submitted.

[31] G. Busca, F. Cavani, G. Centi and F. Trifio, J. Catal. 99 (1986) 400.

[32] J.R. Ebner and M.R. Thompson, Catal. Today 16 (1993) 51.